



ELSEVIER

Contents lists available at ScienceDirect

Comput. Methods Appl. Mech. Engrg.

journal homepage: www.elsevier.com/locate/cma

Consistency and convergence properties of the isogeometric collocation method



Hongwei Lin ^{a,*}, Qianqian Hu ^b, Yunyang Xiong ^a

^a Department of Mathematics, State Key Lab. of CAD&CG, Zhejiang University, Hangzhou 310027, China

^b Department of Mathematics, Zhejiang Gongshang University, Hangzhou 310018, China

ARTICLE INFO

Article history:

Received 3 August 2013

Received in revised form 28 September 2013

Accepted 30 September 2013

Available online 12 October 2013

Keywords:

Isogeometric analysis

Collocation method

Convergence

Consistency

NURBS

ABSTRACT

Isogeometric collocation (IGA-C) method has shown its superior behavior over Galerkin method in terms of accuracy-to-computational-time ratio and other aspects. However, relatively little has been published about numerical analysis of the IGA-C method. This paper develops theoretical results on consistency and convergence of the IGA-C method to a generic boundary (initial) problem. It shows that the IGA-C method is convergent when differential operator of the boundary (initial) problem is stable or strongly monotone. Finally, we show some concrete examples whose differential operators are strongly monotone, and the IGA-C method is convergent. Moreover, 2D and 3D numerical examples are presented.

© 2013 Elsevier B.V. All rights reserved.

1. Introduction

Finite Element Analysis (FEA) gains widespread applications in physical simulation. However, while classical FEA methods are based on linear basis functions, CAD models are usually represented by NURBS with non-linear NURBS basis functions. When performing CAD model simulation, the NURBS-based CAD model should be transformed into linear mesh representation. As we all know, the operation of mesh transformation is very tedious, and it has become the most time-consuming task in the whole FEA procedure. Therefore, isogeometric analysis (IGA) is proposed by Hughes et. al. [1] to avoid the mesh transformation and to advance the seamless integration of CAD and CAE.

Since the IGA method is based on non-linear NURBS basis functions, it can deal with NURBS-based CAD models directly. And the IGA method can not only save lots of computation, but also greatly improve the computational precision. In addition, due to the knot insertion property of NURBS, the shape of CAD model can be exactly held in the refinement procedure [1]. Owing so many merits, the IGA method has been successfully applied in kinds of simulation problems, such as elasticity [2,3], structure [4–6], and fluid [7–9], etc.

For now, some work focuses on computational aspect of the IGA method and improves the accuracy and efficiency by using reparameterization and refinement, etc. [10–15]. Collocation method is a simple and efficient numerical method for solving differential equation, which can generate a numerical solution satisfying the differential equation at a set of discrete points, called collocation points [16]. If an unknown NURBS function is employed to approximate the analytical solution of a differential equation and its order is high enough, the collocation method can be applied to the strong form of the differential equation. Based on this fact, Auricchio et al. proposed the well-known isogeometric collocation (IGA-C) method [17]. For a boundary/initial problem with differential operator \mathcal{D} , we denote by T and T_r the analytic and numerical solutions,

* Corresponding author. Tel.: +86 571 87951860x8304; fax: +86 571 88206681.

E-mail addresses: hwlin@zju.edu.cn, hwlin@zjucadcg.cn (H. Lin).

respectively, and n the number of the unknown coefficients of the NURBS function T_r . The IGA-C method first samples n values $\mathcal{D}T_r(\eta_i)$, $i = 1, 2, \dots, n$, and then generates a system of linear equations by $\mathcal{D}T_r$ interpolating these n values, i.e., $\mathcal{D}T(\eta_i) = \mathcal{D}T_r(\eta_i)$, $i = 1, 2, \dots, n$. The unknown coefficients of T_r can be determined by solving the linear system.

The IGA-C method has been extended to multi-patch NURBS configurations, various boundary and patch interface conditions, and explicit dynamic analysis [18]. Moreover, the IGA-C method has also been successfully employed in solving Timoshenko beam problem [19] and spatial Timoshenko rod problem [20], showing that mixed collocation schemes are locking-free independently of the choice of the polynomial degrees for the unknown fields. A comprehensive study on the IGA-C method reveals its superior behavior over Galerkin method in terms of accuracy-to-computational-time ratio [21]. Meanwhile, adaptive IGA-C methods are also developed and analyzed based on local hierarchical refinement of NURBS [21].

Unfortunately, a thorough numerical analysis of the IGA-C method is far from being established. Till now, all the analysis of the IGA-C method is only available for the one-dimensional case [17]. And the convergence results for 2D and 3D NURBS discretizations are available only based on numerical experiments [17,18].

In this paper, we present some theoretical consistency and convergence results of the IGA-C method for a generic differential operator. We first prove the consistency property of the IGA-C method. That is, for a PDE with the differential operator \mathcal{D} , T is its analytic solution, and a NURBS function T_r is the numerical solution. $\mathcal{D}T_r$ will tend to $\mathcal{D}T$, when each knot interval of T_r tends to a point. Then a theoretical convergence result is presented, and we prove that, if \mathcal{D} is a stable or strongly monotone operator, the numerical solution T_r will tend to the analytic solution T when each knot interval of T_r tends to a point. Finally, we give some concrete examples where the differential operators are strongly monotone, and then the IGA-C method is convergent. It should be pointed out that, while the rate of convergence of the IGA-C method for one-dimensional problems is developed in [17], we just show the convergence of the IGA-C method for higher dimensional problems with stable or strongly monotone operator in this paper. Especially, when the differential operator is a stable or strongly monotone operator with polynomial coefficients, we present an error bound for the numerical solution generated by the IGA-C method.

The rest of this paper is laid out as follows. The generic formula of the IGA-C method is presented in Section 2. In Section 3, we study the knot vector of the derivative of arbitrary order of a NURBS function T_r , and prove that T_r and $\mathcal{D}T_r$ have the same breakpoint sequence and knot intervals. In Section 4, the theoretical consistency and convergence results of the IGA-C method are developed, and some concrete examples and numerical examples are presented. Finally, we conclude this paper in Section 5.

2. Generic formulation of the IGA-C method

A boundary value problem is expressed as

$$\begin{cases} \mathcal{D}T = f, & \text{in } \Omega \subset \mathbb{R}^d, \\ \mathcal{G}T = g, & \text{on } \partial\Omega, \end{cases} \tag{1}$$

where $\Omega \subset \mathbb{R}^d$ is a physical domain of d dimension, \mathcal{D} is a bounded differential operator on the physical domain, $\mathcal{G}T = g$ is a boundary condition, and $f : \Omega \rightarrow \mathbb{R}$, $g : \partial\Omega \rightarrow \mathbb{R}$ are given functions. Suppose k is the maximum order of derivatives appearing in the operator $\mathcal{D} : V \rightarrow W$, where V and W are two Hilbert spaces, and the analytical solution $T \in C^m(\Omega)$, $m \geq k$.

In the isogeometric analysis, the physical domain Ω is represented by a NURBS mapping:

$$\mathbf{F} : \Omega_0 \rightarrow \Omega, \tag{2}$$

where Ω_0 is a parametric domain. Replacing the control points of $\mathbf{F}(\Omega_0)$ by unknown control coefficients, we obtain the representation of numerical solution T_r , where $T_r \in C^k(\Omega)$.

Suppose there are n unknown control coefficients in the representation of T_r . We first sample n_1 points inside Ω_0 , which correspond to n_1 values inside Ω , i.e., $\eta_i = \mathbf{F}(\theta_i)$, $i = 1, 2, \dots, n_1$. Next, we sample n_2 points on $\partial\Omega_0$, which correspond to n_2 values on $\partial\Omega$, i.e., $\eta_i = \mathbf{F}(\theta_i)$, $i = n_1 + 1, n_1 + 2, \dots, n_1 + n_2$. The total number of these points, called *collocation points*, should be equal to the number of the unknown coefficients of T_r , i.e., $n = n_1 + n_2$.

Inserting these collocation points into the boundary value problem (1) yields a system of equations with n equations and n unknowns, i.e.,

$$\begin{cases} \mathcal{D}T_r(\eta_i) = f(\eta_i), & i = 1, 2, \dots, n_1, \\ \mathcal{G}T_r(\eta_i) = g(\eta_i), & i = n_1 + 1, n_1 + 2, \dots, n. \end{cases} \tag{3}$$

Arranging the unknowns of T_r into an n -dimensional column vector, i.e., $X = [x_1 \ x_2 \ \dots \ x_n]^T$, the system of Eq. (3) can be represented in matrix form as

$$AX = b.$$

If the collocation points are so selected that the collocation matrix A is non-singular, the unknown coefficients X can be determined by solving the above mentioned system of linear equations.

3. The knot vector of derivatives of a NURBS function

In the IGA-C method, the numerical solution T_r is a NURBS function, and $\mathcal{D}T_r$ where the differential operator \mathcal{D} is shown as in (1) is composed by derivatives of T_r . In this section, we will show that the derivatives of arbitrary order of a NURBS function T_r have the same knot intervals as T_r , and so does $\mathcal{D}T_r$.

3.1. Univariate NURBS function

We first consider the following univariate NURBS function represented by

$$T_r(u) = \frac{\sum_i N_i(u)\omega_i T_i}{\sum_i N_i(u)\omega_i} \triangleq \frac{P_0(u)}{W_0(u)} \tag{4}$$

of degree h , with control points T_i , the associated weights ω_i , and knot vector

$$\underbrace{u_1, \dots, u_1}_{i_1=h+1}, \underbrace{u_2, \dots, u_2}_{0 < i_2 \leq h+1}, \dots, \underbrace{u_{\alpha-1}, \dots, u_{\alpha-1}}_{0 < i_{\alpha-1} \leq h+1}, \underbrace{u_\alpha, \dots, u_\alpha}_{i_\alpha=h+1}. \tag{5}$$

Breakpoint sequence of the NURBS function $T_r(u)$ (4) is defined as the distinct knot values in ascending order, i.e., $\{u_1, u_2, \dots, u_\alpha\}$.

Since $T_r(u)$ (4) is a rational function, its derivative has the item of product of two spline functions, whose knot vector is presented in the following Lemma 1 [22].

Lemma 1. Given a B-spline function $F(u)$ of degree h_1 defined on knot vector,

$$\underbrace{\xi_1, \dots, \xi_1}_{n_1=h_1+1}, \underbrace{\xi_2, \dots, \xi_2}_{0 < n_2 \leq h_1+1}, \dots, \underbrace{\xi_{r-1}, \dots, \xi_{r-1}}_{0 < n_{r-1} \leq h_1+1}, \underbrace{\xi_r, \dots, \xi_r}_{n_r=h_1+1}$$

and a B-spline function $G(u)$ of degree h_2 defined on knot vector,

$$\underbrace{\delta_1, \dots, \delta_1}_{m_1=h_2+1}, \underbrace{\delta_2, \dots, \delta_2}_{0 < m_2 \leq h_2+1}, \dots, \underbrace{\delta_{s-1}, \dots, \delta_{s-1}}_{0 < m_{s-1} \leq h_2+1}, \underbrace{\delta_s, \dots, \delta_s}_{m_s=h_2+1}$$

the product of $F(u)$ and $G(u)$ is a spline function of degree $H = h_1 + h_2$ defined on knot vector,

$$\underbrace{\mu_1, \dots, \mu_1}_{l_1=H+1}, \underbrace{\mu_2, \dots, \mu_2}_{0 < l_2 \leq H+1}, \dots, \underbrace{\mu_{t-1}, \dots, \mu_{t-1}}_{0 < l_{t-1} \leq H+1}, \underbrace{\mu_t, \dots, \mu_t}_{l_t=H+1}.$$

For $0 < i < t$, the multiplicity of μ_i is computed according to Table 1.

Then, we have the following theorem.

Theorem 1. The n th-order derivative of the NURBS function $T_r(u)$ (4) can be written as

$$T_r^{(n)}(u) = \frac{P_n(u)}{W_n(u)},$$

where $P_n(u)$ is a spline function of degree $(2^n h - n)$, with knot vector

$$\underbrace{u_1, \dots, u_1}_{2^n h - n + 1}, \underbrace{u_2, \dots, u_2}_{i_2 + (2^n - 1)h}, \dots, \underbrace{u_{\alpha-1}, \dots, u_{\alpha-1}}_{i_{\alpha-1} + (2^n - 1)h}, \underbrace{u_\alpha, \dots, u_\alpha}_{2^n h - n + 1}$$

and the breakpoint sequence $\{u_1, u_2, \dots, u_\alpha\}$; $W_n(u)$ is a spline function of degree $2^n h$, with knot vector

$$\underbrace{u_1, \dots, u_1}_{2^n h + 1}, \underbrace{u_2, \dots, u_2}_{i_2 + (2^n - 1)h}, \dots, \underbrace{u_{\alpha-1}, \dots, u_{\alpha-1}}_{i_{\alpha-1} + (2^n - 1)h}, \underbrace{u_\alpha, \dots, u_\alpha}_{2^n h + 1}$$

and the breakpoint sequence $\{u_1, u_2, \dots, u_\alpha\}$. In other words, $T_r(u)$ and its n th-order derivative $T_r^{(n)}(u)$ have the same breakpoint sequence $\{u_1, u_2, \dots, u_\alpha\}$.

Proof. Here mathematical induction is used to prove the theorem.

Table 1
Multiplicity of μ_i ($0 < i < t$).

| | | |
|---|------------------------------------|---|
| 1 | $l_i = n_j + h_2$ | If $\mu_i = \xi_j$ for some j but is absent from $G(u)$'s knot vector |
| 2 | $l_i = m_k + h_1$ | If $\mu_i = \delta_k$ for some k but is absent from $F(u)$'s knot vector |
| 3 | $l_i = \max(n_j + h_2, m_k + h_1)$ | If $\mu_i = \xi_j = \delta_k$ for some j and k |

Deriving $T_r(u)$ (4) with respect to u yields

$$T'_r(u) = \frac{P'_0(u)W_0(u) - P_0(u)W'_0(u)}{W_0^2(u)} \triangleq \frac{P_1(u)}{W_1(u)}. \tag{6}$$

这个微分算子必须是个线性算子，如果是个非线性算子，则会出现一个关于NURBS函数未知系数的非线性方程组。

According to (4), the h -degree spline functions $P_0(u)$ and $W_0(u)$ are defined on the knot vector (5). It is easy to show that $P'_0(u)$ and $W'_0(u)$ are both defined on

$$\underbrace{u_1, \dots, u_1}_h, \underbrace{u_2, \dots, u_2}_{0 < i_2 \leq h+1}, \dots, \underbrace{u_{\alpha-1}, \dots, u_{\alpha-1}}_{0 < i_{\alpha-1} \leq h+1}, \underbrace{u_\alpha, \dots, u_\alpha}_h$$

and their degree is $(h - 1)$. Based on Lemma 1, $P_1(u)$ in (6) is defined on knot vector

$$\underbrace{u_1, \dots, u_1}_{2h}, \underbrace{u_2, \dots, u_2}_{i_2+h}, \dots, \underbrace{u_{\alpha-1}, \dots, u_{\alpha-1}}_{i_{\alpha-1}+h}, \underbrace{u_\alpha, \dots, u_\alpha}_{2h}$$

and its degree is $(2h - 1)$. On the other hand, $W_1(u) = W_0^2(u)$ is defined on knot vector

$$\underbrace{u_1, \dots, u_1}_{2h+1}, \underbrace{u_2, \dots, u_2}_{i_2+h}, \dots, \underbrace{u_{\alpha-1}, \dots, u_{\alpha-1}}_{i_{\alpha-1}+h}, \underbrace{u_\alpha, \dots, u_\alpha}_{2h+1}$$

and its degree is $2h$. Therefore, the statement holds for $n = 1$.

Assume that the statement holds for some unspecified value of $n - 1$, $n \geq 2$. That is,

$$T_r^{(n-1)}(u) = \frac{P_{n-1}(u)}{W_{n-1}(u)}, \tag{7}$$

where $P_{n-1}(u)$ is a $(2^{n-1}h - n + 1)$ -degree spline function with knot vector

$$\underbrace{u_1, \dots, u_1}_{2^{n-1}h-n+2}, \underbrace{u_2, \dots, u_2}_{i_2+(2^{n-1}-1)h}, \dots, \underbrace{u_{\alpha-1}, \dots, u_{\alpha-1}}_{i_{\alpha-1}+(2^{n-1}-1)h}, \underbrace{u_\alpha, \dots, u_\alpha}_{2^{n-1}h-n+2}$$

$W_{n-1}(u)$ is a $2^{n-1}h$ -degree spline function with knot vector

$$\underbrace{u_1, \dots, u_1}_{2^{n-1}h+1}, \underbrace{u_2, \dots, u_2}_{i_2+(2^{n-1}-1)h}, \dots, \underbrace{u_{\alpha-1}, \dots, u_{\alpha-1}}_{i_{\alpha-1}+(2^{n-1}-1)h}, \underbrace{u_\alpha, \dots, u_\alpha}_{2^{n-1}h+1}$$

Deriving $T_r^{(n-1)}(u)$ (7) with respect to u yields

$$T_r^{(n)}(u) = \frac{P'_{n-1}(u)W_{n-1}(u) - P_{n-1}(u)W'_{n-1}(u)}{W_{n-1}^2(u)} \triangleq \frac{P_n(u)}{W_n(u)}.$$

Also based on Lemma 1, $P'_{n-1}(u)W_{n-1}(u)$ is a $(2^n h - n)$ -degree spline function defined on

$$\underbrace{u_1, \dots, u_1}_{2^n h-n+1}, \underbrace{u_2, \dots, u_2}_{i_2+(2^n-1)h}, \dots, \underbrace{u_{\alpha-1}, \dots, u_{\alpha-1}}_{i_{\alpha-1}+(2^n-1)h}, \underbrace{u_\alpha, \dots, u_\alpha}_{2^n h-n+1} \tag{8}$$

$P_{n-1}(u)W'_{n-1}(u)$ is a $(2^n h - n)$ -degree spline function defined on

$$\underbrace{u_1, \dots, u_1}_{2^n h-n+1}, \underbrace{u_2, \dots, u_2}_{i_2+(2^n-1)h-1}, \dots, \underbrace{u_{\alpha-1}, \dots, u_{\alpha-1}}_{i_{\alpha-1}+(2^n-1)h-1}, \underbrace{u_\alpha, \dots, u_\alpha}_{2^n h-n+1} \tag{9}$$

By inserting $u_2, u_3, \dots, u_{\alpha-1}$ into the knot vector (9) using the de Boor algorithm, both knot vectors (8) and (9) are identical. Therefore, $P_n(u) = P'_{n-1}(u)W_{n-1}(u) - P_{n-1}(u)W'_{n-1}(u)$ is a spline function of degree $(2^n h - n)$ with the knot vector (8).

On the other hand, $W_n(u) = W_{n-1}^2(u)$ is a $2^n h$ -degree spline function defined on knot vector

$$\underbrace{u_1, \dots, u_1}_{2^n h+1}, \underbrace{u_2, \dots, u_2}_{i_2+(2^n-1)h}, \dots, \underbrace{u_{\alpha-1}, \dots, u_{\alpha-1}}_{i_{\alpha-1}+(2^n-1)h}, \underbrace{u_\alpha, \dots, u_\alpha}_{2^n h+1}$$

Therefore, it is shown that indeed the statement holds for n . Since both the basic and the inductive steps have been proved, then the statement holds for all n . And the theorem is proved. \square

According to Theorem 1, the NURBS function $T_r(u)$ (4) and its derivatives of arbitrary order have the same breakpoint sequence $\{u_1, u_2, \dots, u_\alpha\}$. Since $\mathcal{D}T_r(u)$ is a combination of $T_r(u)$ and its derivatives, $\mathcal{D}T_r(u)$ has the same breakpoint sequence as $T_r(u)$ and its derivatives of arbitrary order. Therefore, they are defined on the same knot intervals, i.e.,

Corollary 1. The NURBS function $T_r(u)$ (4), its derivatives of arbitrary order, and $\mathcal{D}T_r(u)$ are defined on the same knot intervals,

$$[u_1, u_2], [u_2, u_3], \dots, [u_{\alpha-1}, u_\alpha].$$

Remark 1. The order n of the derivative of $T_r(u)$ (4) is not more than the minimum of $h - i_s$, $s = 2, 3, \dots, \alpha - 1$, i.e.,

$$n \leq \min_{2 \leq s \leq \alpha-1} \{h - i_s\},$$

since the multiplicity of an inner knot cannot exceed the degree of a NURBS function.

3.2. Bivariate and trivariate NURBS functions

Next, we consider the case of bivariate NURBS functions. Suppose numerical solution $T_r(u, v)$ is represented by a bivariate NURBS function of degree $h \times g$,

$$T_r(u, v) = \frac{\sum_{i,j} N_i(u)N_j(v)\omega_{ij}T_{ij}}{\sum_{i,j} N_i(u)N_j(v)\omega_{ij}}, \tag{10}$$

where T_{ij} are control coefficients, and ω_{ij} are the associated weights. It is defined on knot vectors

$$\underbrace{u_1, \dots, u_1}_{i_1=h+1}, \underbrace{u_2, \dots, u_2}_{0 < i_2 \leq h+1}, \dots, \underbrace{u_{\alpha-1}, \dots, u_{\alpha-1}}_{0 < i_{\alpha-1} \leq h+1}, \dots, \underbrace{u_{\alpha}, \dots, u_{\alpha}}_{i_{\alpha}=h+1},$$

$$\underbrace{v_1, \dots, v_1}_{j_1=g+1}, \underbrace{v_2, \dots, v_2}_{0 < j_2 \leq g+1}, \dots, \underbrace{v_{\beta-1}, \dots, v_{\beta-1}}_{0 < j_{\beta-1} \leq g+1}, \dots, \underbrace{v_{\beta}, \dots, v_{\beta}}_{j_{\beta}=g+1}$$

and its breakpoint sequences are $\{u_1, u_2, \dots, u_{\alpha}\}$ and $\{v_1, v_2, \dots, v_{\beta}\}$.

At first, we give a lemma to elucidate knot vectors of the product of two bivariate B-spline functions.

Lemma 2. Given a bivariate B-spline function $F(u, v)$ of degree $h_1 \times g_1$, i.e.,

$$F(u, v) = \sum_i \sum_j N_i(u)N_j(v)F_{ij},$$

defined on knot vectors

$$\underbrace{\xi_1, \dots, \xi_1}_{n_1=h_1+1}, \underbrace{\xi_2, \dots, \xi_2}_{0 < n_2 \leq h_1+1}, \dots, \underbrace{\xi_{r-1}, \dots, \xi_{r-1}}_{0 < n_{r-1} \leq h_1+1}, \underbrace{\xi_r, \dots, \xi_r}_{n_r=h_1+1},$$

$$\underbrace{\lambda_1, \dots, \lambda_1}_{\bar{n}_1=g_1+1}, \underbrace{\lambda_2, \dots, \lambda_2}_{0 < \bar{n}_2 \leq g_1+1}, \dots, \underbrace{\lambda_{\bar{r}-1}, \dots, \lambda_{\bar{r}-1}}_{0 < \bar{n}_{\bar{r}-1} \leq g_1+1}, \underbrace{\lambda_{\bar{r}}, \dots, \lambda_{\bar{r}}}_{\bar{n}_{\bar{r}}=g_1+1}$$

and a bivariate B-spline function $G(u, v)$ of degree $h_2 \times g_2$, i.e.,

$$G(u, v) = \sum_i \sum_j N_i(u)N_j(v)G_{ij},$$

defined on knot vectors

$$\underbrace{\delta_1, \dots, \delta_1}_{m_1=h_2+1}, \underbrace{\delta_2, \dots, \delta_2}_{0 < m_2 \leq h_2+1}, \dots, \underbrace{\delta_{s-1}, \dots, \delta_{s-1}}_{0 < m_{s-1} \leq h_2+1}, \underbrace{\delta_s, \dots, \delta_s}_{m_s=h_2+1},$$

$$\underbrace{\phi_1, \dots, \phi_1}_{\bar{m}_1=g_2+1}, \underbrace{\phi_2, \dots, \phi_2}_{0 < \bar{m}_2 \leq g_2+1}, \dots, \underbrace{\phi_{\bar{s}-1}, \dots, \phi_{\bar{s}-1}}_{0 < \bar{m}_{\bar{s}-1} \leq g_2+1}, \underbrace{\phi_{\bar{s}}, \dots, \phi_{\bar{s}}}_{\bar{m}_{\bar{s}}=g_2+1}.$$

The product of $F(u, v)$ and $G(u, v)$ is a bivariate spline function of degree $H \times G$, with u -directional knot vector

$$\underbrace{\mu_1, \dots, \mu_1}_{l_1=H+1}, \underbrace{\mu_2, \dots, \mu_2}_{0 < l_2 \leq H+1}, \dots, \underbrace{\mu_{t-1}, \dots, \mu_{t-1}}_{0 < l_{t-1} \leq H+1}, \underbrace{\mu_t, \dots, \mu_t}_{l_t=H+1}, \tag{11}$$

where $H = h_1 + h_2$, and v -directional knot vector

$$\underbrace{v_1, \dots, v_1}_{\bar{l}_1=G+1}, \underbrace{v_2, \dots, v_2}_{0 < \bar{l}_2 \leq G+1}, \dots, \underbrace{v_{\bar{t}-1}, \dots, v_{\bar{t}-1}}_{0 < \bar{l}_{\bar{t}-1} \leq G+1}, \underbrace{v_{\bar{t}}, \dots, v_{\bar{t}}}_{\bar{l}_{\bar{t}}=G+1}, \tag{12}$$

where $G = g_1 + g_2$. For $0 < i < t$, the multiplicity of μ_i is computed according to Table 2; for $0 < i < \bar{t}$, the multiplicity of v_i is computed according to Table 3.

Table 2
Multiplicity of μ_i , ($0 < i < t$).

| | | |
|---|------------------------------------|--|
| 1 | $l_i = n_j + h_2$ | If $\mu_i = \xi_j$ for some j but is absent from $G(u, v)$'s knot vector |
| 2 | $l_i = m_k + h_1$ | If $\mu_i = \delta_k$ for some k but is absent from $F(u, v)$'s knot vector |
| 3 | $l_i = \max(n_j + h_2, m_k + h_1)$ | If $\mu_i = \xi_j = \delta_k$ for some j and k |

Proof. Denote by $H(u, v)$ the product of $F(u, v)$ and $G(u, v)$, i.e., $H(u, v) = F(u, v)G(u, v)$. We fix $v = \bar{v}$ to generate the u -directional knot vector of $H(u, v)$. So,

$$H(u, \bar{v}) = F(u, \bar{v})G(u, \bar{v}) = \sum_i N_i(u) \left(\sum_j N_j(\bar{v}) F_{ij} \right) \cdot \sum_i N_i(u) \left(\sum_j N_j(\bar{v}) G_{ij} \right).$$

Obviously, $F(u, \bar{v})$ is a univariate B-spline function of degree h_1 , $G(u, \bar{v})$ is a univariate B-spline function of degree h_2 , and $H(u, \bar{v})$ is the product of these two univariate B-spline functions. Then based on Lemma 1, $H(u, \bar{v})$ is a B-spline function of degree $(h_1 + h_2)$, defined on the knot vector (11).

Similarly, by fixing $u = \bar{u}$, we can also show that $H(\bar{u}, v)$ is a B-spline function of degree $(g_1 + g_2)$, defined on the knot vector (12).

In conclusion, $H(u, v)$ is a bivariate B-spline function of degree $(h_1 + h_2) \times (g_1 + g_2)$, defined on the knot vectors (11) and (12). □

Theorem 2. The partial derivative of arbitrary order of the bivariate NURBS function $T_r(u, v)$ (10), i.e., $\frac{\partial^{i+j} T_r(u, v)}{\partial u^i \partial v^j}$, where

$$i \leq \min_{2 \leq s \leq \alpha-1} \{h - i_s\}, \quad j \leq \min_{2 \leq s \leq \beta-1} \{g - j_s\}$$

has the same breakpoint sequence as $T_r(u, v)$, i.e.,

$$\{u_1, u_2, \dots, u_\alpha\} \text{ and } \{v_1, v_2, \dots, v_\beta\}$$

and so does $\mathcal{D}T_r(u, v)$ where \mathcal{D} is defined in (1). Therefore, $T_r(u, v)$, its partial derivatives of arbitrary order, and $\mathcal{D}T_r(u, v)$ are all defined on the same knot intervals.

Similar to the proof of Theorem 1, Theorem 2 can be proved by mathematical induction based on Lemma 2.

Moreover, we have similar result to a trivariate NURBS function $T_r(u, v, w)$ of degree $h \times g \times f$, i.e.,

$$T_r(u, v, w) = \frac{\sum_{i,j,k} N_i(u) N_j(v) N_k(w) \omega_{ijk} T_{ijk}}{\sum_{i,j,k} N_i(u) N_j(v) N_k(w) \omega_{ijk}}, \tag{13}$$

where T_{ijk} are control coefficients, and ω_{ijk} are the associated weights. It is defined on knot vectors

$$\underbrace{u_1, \dots, u_1}_{i_1=h+1}, \underbrace{u_2, \dots, u_2}_{0 < i_2 \leq h+1}, \dots, \underbrace{u_{\alpha-1}, \dots, u_{\alpha-1}}_{0 < i_{\alpha-1} \leq h+1}, \dots, \underbrace{u_\alpha, \dots, u_\alpha}_{i_\alpha=h+1},$$

$$\underbrace{v_1, \dots, v_1}_{j_1=g+1}, \underbrace{v_2, \dots, v_2}_{0 < j_2 \leq g+1}, \dots, \underbrace{v_{\beta-1}, \dots, v_{\beta-1}}_{0 < j_{\beta-1} \leq g+1}, \dots, \underbrace{v_\beta, \dots, v_\beta}_{j_\beta=g+1},$$

$$\underbrace{w_1, \dots, w_1}_{k_1=f+1}, \underbrace{w_2, \dots, w_2}_{0 < k_2 \leq f+1}, \dots, \underbrace{w_{\gamma-1}, \dots, w_{\gamma-1}}_{0 < k_{\gamma-1} \leq f+1}, \dots, \underbrace{w_\gamma, \dots, w_\gamma}_{k_\gamma=f+1}.$$

Theorem 3. The partial derivative of arbitrary order of the trivariate NURBS function $T_r(u, v, w)$, i.e., $\frac{\partial^{i+j+k} T_r(u, v, w)}{\partial u^i \partial v^j \partial w^k}$, where

$$i \leq \min_{2 \leq s \leq \alpha-1} \{h - i_s\}, \quad j \leq \min_{2 \leq s \leq \beta-1} \{g - j_s\}, \quad k \leq \min_{2 \leq s \leq \gamma-1} \{f - k_s\}$$

has the same breakpoint sequence as $T_r(u, v, w)$, and so does $\mathcal{D}T_r(u, v, w)$. Therefore, $T_r(u, v, w)$, its partial derivative of arbitrary order, and $\mathcal{D}T_r(u, v, w)$ are all defined on the same knot intervals.

Remark 2. Evidently, the result in the above theorem is held for higher dimensional NURBS function.

Table 3
Multiplicity of v_i , ($0 < i < t$).

| | | |
|---|--|---|
| 1 | $\bar{l}_i = \bar{n}_j + g_2$ | If $v_i = \lambda_j$ for some j but is absent from $G(u, v)$'s knot vector |
| 2 | $\bar{l}_i = \bar{m}_k + g_1$ | If $v_i = \phi_k$ for some k but is absent from $F(u, v)$'s knot vector |
| 3 | $\bar{l}_i = \max(\bar{n}_j + g_2, \bar{m}_k + g_1)$ | If $v_i = \lambda_j = \phi_k$ for some j and k |

4. Main results

In this section, we will develop the main results of this paper, i.e., the theoretical consistency and convergence properties of the IGA-C method, in Sections 4.1 and 4.2, respectively. Moreover, some concrete examples with strongly monotone operator and some numerical examples are presented in Section 4.3.

4.1. Consistency

Definition 1. Given a set $\Phi \subset \mathbb{R}^d$, its **diameter** $diam(\Phi)$ is defined as

$$diam(\Phi) = \sup\{d(x, y), x, y \in \Phi\},$$

where $d(x, y)$ denotes the Euclidean distance between x and y . Moreover, we call ρ as *knot grid size*, which is defined as the maximum of the diameters of the knot intervals. That is, $\rho = \max_i\{diam([u_i, u_{i+1}])\}$ in 1D case, $\rho = \max_{ij}\{diam([u_i, u_{i+1}] \times [v_j, v_{j+1}])\}$ in 2D case, and $\rho = \max_{ijk}\{diam([u_i, u_{i+1}] \times [v_j, v_{j+1}] \times [w_k, w_{k+1}])\}$ in 3D case.

When the approximate differential expression \mathcal{DT}_r interpolates the real differential expression \mathcal{DT} at some collocation points, we have the following results.

Theorem 4 (One dimensional case). *Suppose the numerical solution to the boundary value problem (1) is represented by the NURBS function $T_r(u)$ (4), and there is at least one collocation point η_i in the knot interval $[u_i, u_{i+1}]$, $i = 1, \dots, \alpha - 1$. If the approximate differential expression $\mathcal{DT}_r(u)$ interpolates the values of the real differential expression $\mathcal{DT}(u)$ at the collocation points $\eta_i \in [u_i, u_{i+1}]$, $i = 1, \dots, \alpha - 1$, i.e., $\mathcal{DT}(\eta_i) = \mathcal{DT}_r(\eta_i)$, and $T_r(u)$ satisfies the local Lipschitz condition, i.e.,*

$$\exists \delta > 0, \forall \xi_1, \xi_2 \in [u_1, u_\alpha], |\xi_1 - \xi_2| < \delta, \text{ we have } |T_r(\xi_1) - T_r(\xi_2)| < K|\xi_1 - \xi_2|, \text{ for any } \rho \rightarrow 0,$$

where $K > 0$ is a constant and ρ is the knot grid size defined in Definition 1, then $\mathcal{DT}_r(u)$ will tend to $\mathcal{DT}(u)$ in the L^∞ norm, when the length of each knot interval of $T_r(u)$ tends to 0, i.e., $\rho \rightarrow 0$.

Proof. Based on Theorem 1 and Corollary 1, $\mathcal{DT}_r(u)$ and $T_r(u)$ are defined on the same knot intervals, $[u_i, u_{i+1}]$, $i = 1, \dots, \alpha - 1$.

Denote $r(u) = \mathcal{DT}(u) - \mathcal{DT}_r(u)$, and suppose $\hat{u} \in [u_i, u_{i+1}]$. Due to the Lagrange's mean value theorem, we have,

$$\frac{r(\hat{u}) - r(\eta_i)}{\hat{u} - \eta_i} = \frac{r(\hat{u})}{\hat{u} - \eta_i} = r'(\xi),$$

where $\xi \in (\min(\eta_i, \hat{u}), \max(\eta_i, \hat{u}))$. Therefore,

$$|r(\hat{u})| = |r'(\xi)(\hat{u} - \eta_i)| \leq \max_{\xi \in [u_i, u_{i+1}]} |r'(\xi)| \max_i (u_{i+1} - u_i).$$

Since \hat{u} is an arbitrary value in $[u_i, u_{i+1}]$, we have,

$$\|\mathcal{DT}(u) - \mathcal{DT}_r(u)\|_{L^\infty} = \|r(u)\|_{L^\infty} \leq \max_i \max_{\xi \in [u_i, u_{i+1}]} |r'(\xi)| \max_i (u_{i+1} - u_i) \leq \rho \|r'(u)\|_{L^\infty}. \tag{14}$$

On the other hand, noting that $T_r(u)$ satisfies the local Lipschitz condition, the derivative of $T_r(u)$ is bounded for $\rho \rightarrow 0$, i.e.,

$$|T'_r(u)| = \lim_{\Delta u \rightarrow 0} \frac{|T_r(u + \Delta u) - T_r(u)|}{|\Delta u|} \leq \lim_{\Delta u \rightarrow 0} \frac{K|\Delta u|}{|\Delta u|} = K.$$

Then we have,

$$\|\mathcal{DT}'_r(u)\|_{L^\infty} \leq \|\mathcal{D}\|_{V'} \|T'_r(u)\|_{L^\infty} \leq K \|\mathcal{D}\|_{V'}, \text{ for any } \rho \rightarrow 0,$$

where $\|\cdot\|_{V'}$ is the norm in the dual space V' . It means that, $\|r'(u)\|_{L^\infty}$ is also bounded for any $\rho \rightarrow 0$.

Therefore, according to (14), $\|r(u)\|_{L^\infty}$ tends to 0, when the lengths of knot intervals of $T_r(u)$ tend to 0, i.e., $\rho \rightarrow 0$. And the theorem is proved. \square

The following theorem deals with the two dimensional case.

Theorem 5 (Two dimensional case). *Suppose the numerical solution to the boundary value problem (1) is represented by the bivariate NURBS function $T_r(u, v)$ (10), and there is at least one collocation point $\boldsymbol{\eta}_{ij} = (\mu_{ij}, \nu_{ij})$ in the knot interval $[u_i, u_{i+1}] \times [v_j, v_{j+1}]$, $i = 1, \dots, \alpha - 1$, $j = 1, \dots, \beta - 1$. If the approximate differential expression $\mathcal{DT}_r(u, v)$ interpolates the values of the real differential expression $\mathcal{DT}(u, v)$ at the following collocation points*

$$\boldsymbol{\eta}_{ij} \in [u_i, u_{i+1}] \times [v_j, v_{j+1}], \quad i = 1, \dots, \alpha - 1, \quad j = 1, \dots, \beta - 1,$$

i.e., $\mathcal{D}T(\boldsymbol{\eta}_{ij}) = \mathcal{D}T_r(\boldsymbol{\eta}_{ij})$, and $T_r(u, v)$ satisfies the local Lipschitz condition, i.e.,

$$\exists \delta > 0, \forall \xi_1, \xi_2 \in [u_1, u_\alpha] \times [v_1, v_\beta], d(\xi_1, \xi_2) < \delta, \text{ we have } |T_r(\xi_1) - T_r(\xi_2)| < Kd(\xi_1, \xi_2), \text{ for any } \rho \rightarrow 0,$$

where $K > 0$ is a constant, ρ is the knot grid size defined in Definition 1, and $d(\xi_1, \xi_2)$ is the Euclidean distance between ξ_1 and ξ_2 , then $\mathcal{D}T_r(u, v)$ will tend to $\mathcal{D}T(u, v)$ in the L^∞ norm, when each knot interval $[u_i, u_{i+1}] \times [v_j, v_{j+1}]$ of $T_r(u, v)$ tends to a point, i.e., $\rho \rightarrow 0$.

Proof. Due to Theorem 2, $\mathcal{D}T_r(u, v)$ has the same knot intervals as the bivariate NURBS function $T_r(u, v)$ (10), i.e., $[u_i, u_{i+1}] \times [v_j, v_{j+1}]$, $i = 1, \dots, \alpha - 1$, $j = 1, \dots, \beta - 1$.

Denote $r(u, v) = \mathcal{D}T(u, v) - \mathcal{D}T_r(u, v)$, and suppose $\zeta = (\hat{u}, \hat{v}) \in [u_i, u_{i+1}] \times [v_j, v_{j+1}]$. Based on the mean value theorem in multiple variables, we have

$$r(\zeta) = r(\zeta) - r(\boldsymbol{\eta}_{ij}) = \nabla r|_{(1-c)\zeta+c\boldsymbol{\eta}_{ij}} \cdot (\zeta - \boldsymbol{\eta}_{ij}),$$

where $c \in (0, 1)$, and “ \cdot ” represents inner product.

Thus, we have

$$\|r(\zeta)\|_{L^\infty} \leq \|\nabla r\|_{L^\infty} \left\| \zeta - \boldsymbol{\eta}_{ij} \right\|_{L^\infty} \leq \|\nabla r\|_{L^\infty} \max_{ij} (|u_{i+1} - u_i| + |v_{j+1} - v_j|)$$

and further,

$$\|\mathcal{D}T(\zeta) - \mathcal{D}T_r(\zeta)\|_{L^\infty} = \|r(\zeta)\|_{L^\infty} \leq \|\nabla r\|_{L^\infty} \max_{ij} (|u_{i+1} - u_i| + |v_{j+1} - v_j|) \leq 2\rho \|\nabla r\|_{L^\infty}.$$

Since $T_r(u, v)$ satisfies the local Lipschitz condition, its partial derivatives are bounded, as well as the partial derivatives of $\mathcal{D}T_r(u, v)$. So $\|\nabla r\|_{L^\infty}$ is bounded. According to the above mentioned inequality, the approximate differential expression $\mathcal{D}T_r(u, v)$ will converge to the real differential expression $\mathcal{D}T(u, v)$, when the knot interval $[u_i, u_{i+1}] \times [v_j, v_{j+1}]$ tends to a point, i.e., $\rho \rightarrow 0$. \square

Three dimensional case is handled in a similar fashion, and we have,

Theorem 6 (Three dimensional case). Suppose the numerical solution to the boundary value problem (1) is represented by the trivariate NURBS function $T_r(u, v, w)$ (13), and there is at least one collocation point $\boldsymbol{\eta}_{ijk} = (\mu_{ijk}, \nu_{ijk}, \xi_{ijk})$ in the knot interval $[u_i, u_{i+1}] \times [v_j, v_{j+1}] \times [w_k, w_{k+1}]$, $i = 1, \dots, \alpha - 1$, $j = 1, \dots, \beta - 1$, $k = 1, \dots, \gamma - 1$. If the approximate differential expression $\mathcal{D}T_r(u, v, w)$ interpolates the values of the real differential expression $\mathcal{D}T(u, v, w)$ at the collocation points,

$$\boldsymbol{\eta}_{ijk} \in [u_i, u_{i+1}] \times [v_j, v_{j+1}] \times [w_k, w_{k+1}], \quad i = 1, \dots, \alpha - 1, \quad j = 1, \dots, \beta - 1, \quad k = 1, \dots, \gamma - 1,$$

i.e., $\mathcal{D}T(\boldsymbol{\eta}_{ijk}) = \mathcal{D}T_r(\boldsymbol{\eta}_{ijk})$, and $T_r(u, v, w)$ satisfies the local Lipschitz condition, $\mathcal{D}T_r(u, v, w)$ will tend to $\mathcal{D}T(u, v, w)$ in the L^∞ norm when $\rho \rightarrow 0$, which is defined in Definition 1.

Proof of Theorem 6 is similar to that of Theorem 5.

Especially, when \mathcal{D} is a differential operator with polynomials as coefficients, we can get the error bound of $\|\mathcal{D}T - \mathcal{D}T_r\|_{L^\infty}$. To this end, we need the following Lemma 3.

Suppose \mathcal{T}^ρ is a knot grid on $\Omega_0 \in \mathbb{R}^d$, $d = 1, 2, 3$, e.g., \mathcal{T}^ρ is a knot sequence in 1D case, a rectangular grid in 2D case, and a hexahedral grid in 3D case, where ρ is the knot grid size defined in Definition 1. Let $u \in W_p^m(\Omega_0)$ be a function defined on Ω_0 , where $W_p^m(\Omega_0)$ is a Sobolev space, and $\mathcal{I}^\rho u \in C^0(\Omega_0)$ be a polynomial spline interpolant of u defined on the knot grid \mathcal{T}^ρ . In 1D case, $\mathcal{I}^\rho u$ is a univariate spline function, and in 2D and 3D cases, $\mathcal{I}^\rho u$ is a tensor product spline function. We have the error bound for the interpolant $\mathcal{I}^\rho u$ as follows (refer to p.110 and p. 115 of [23]).

Lemma 3. The error bound for the polynomial spline interpolant $\mathcal{I}^\rho u$ of u defined on the knot grid \mathcal{T}^ρ is,

$$\|u - \mathcal{I}^\rho u\|_{L^\infty} \leq C_T \rho^{m-d/p},$$

where $C_T > 0$ is a constant independent of the knot grid size ρ .

Denote by T_r the numerical solution to the PDE problem (1), expressed as

$$T_r(\zeta) = \frac{P_0(\zeta)}{W_0(\zeta)}, \quad \zeta \in \Omega_0 \subset \mathbb{R}^d, \quad d = 1, 2, 3, \tag{15}$$

where $W_0(\zeta)$ is a known polynomial spline function and $P_0(\zeta)$ is a polynomial spline function with unknown coefficients, which can be solved by the IGA-C method. In 1D case, $P_0(\zeta)$ and $W_0(\zeta)$ are univariate spline functions; in 2D and 3D cases, they are tensor product spline functions.

Suppose the analytical solution T to the problem (1) is transformed into the parametric domain Ω_0 by function composition $T(\mathbf{F}(\Omega_0))$, where \mathbf{F} is defined as in (2). We still denote $T(\mathbf{F}(\Omega_0))$ as T . Accordingly, \mathcal{D} becomes a differential operator defined on the parametric domain Ω_0 . The numerical solution T_r (15) will approximate the analytical solution T defined on Ω_0 .

First, the coefficients of \mathcal{D} are polynomials. By compounding the NURBS mapping $\mathbf{F}(\zeta)$ (2), each polynomial becomes a linear combination of the powers of components of $\mathbf{F}(\zeta)$, i.e., $F(\zeta) = x(u)$ in 1D case, $\mathbf{F}(\zeta) = (x(u, v), y(u, v))$ in 2D case, and $\mathbf{F}(\zeta) = (x(u, v, w), y(u, v, w), z(u, v, w))$ in 3D case. The components x, y, z of $\mathbf{F}(\zeta)$ are known NURBS functions.

Second, in computing the (partial) derivatives of T_r to the variables in the physical domain Ω by chain rule with the inverse mapping $\mathbf{F}^{-1} : \Omega \rightarrow \Omega_0$, extra coefficients will appear in front of the (partial) derivatives of T_r to the corresponding variables in the parametric domain Ω_0 . Each of these coefficients can be obtained by finite time calculations of four rules (i.e., addition, subtraction, multiplication and division) of the (partial) derivatives of components of $\mathbf{F}(\zeta)$, which are known NURBS functions as aforementioned.

Therefore, $\mathcal{D}T_r(\zeta)$, $\zeta \in \Omega_0$ on the parametric domain Ω_0 is the sum of products of NURBS functions and their (partial) derivatives, i.e., the components of $\mathbf{F}(\zeta)$, $T_r(\zeta)$, and their (partial) derivatives. According to Lemmas 1, 2, and Theorems 1,2,3, they have the same breakpoint sequence as $\mathbf{F}(\zeta)$ and $T_r(\zeta)$. Thus, by suitable knot insertion and like item merging, $\mathcal{D}T_r(\zeta)$ can be written as,

$$\mathcal{D}T_r(\zeta) = \frac{P_k(\zeta)}{W_k(\zeta)},$$

where $W_k(\zeta)$ is a known polynomial spline function, and $P_k(\zeta)$ is a polynomial spline function containing the unknown coefficients of $T_r(\zeta)$. $P_k(\zeta)$ and $W_k(\zeta)$ have the same breakpoint sequence as $\mathbf{F}(\zeta)$ and $T_r(\zeta)$. Here, it is supposed that the knots of $P_k(\zeta)$ and $W_k(\zeta)$ are all regular.

According to the above mentioned equation, we have

$$\mathcal{D}T(\zeta) - \mathcal{D}T_r(\zeta) = \frac{W_k(\zeta)\mathcal{D}T(\zeta) - P_k(\zeta)}{W_k(\zeta)}.$$

Thus, the interpolation of $\mathcal{D}T_r(\zeta)$ to $\mathcal{D}T(\zeta)$ becomes to the interpolation of the polynomial spline $P_k(\zeta)$ to $W_k(\zeta)\mathcal{D}T(\zeta)$. Suppose $W_k(\zeta)\mathcal{D}T(\zeta) \in W_p^m(\Omega_0)$. Due to Lemma 3, it holds

$$\|W_k(\zeta)\mathcal{D}T(\zeta) - P_k(\zeta)\|_{L^\infty} \leq C_I \rho^{m-d/p},$$

where ρ is the knot grid size of T^ρ which $T_r(\zeta)$ is defined on. Then we have

$$\|\mathcal{D}T(\zeta) - \mathcal{D}T_r(\zeta)\|_{L^\infty} = \left\| \frac{W_k(\zeta)\mathcal{D}T(\zeta) - P_k(\zeta)}{W_k(\zeta)} \right\|_{L^\infty} \leq \|W_k(\zeta)\mathcal{D}T(\zeta) - P_k(\zeta)\|_{L^\infty} \left\| \frac{1}{W_k(\zeta)} \right\|_{L^\infty} \leq C_I \rho^{m-d/p} \left\| \frac{1}{W_k(\zeta)} \right\|_{L^\infty}.$$

This leads to the following Theorem.

Theorem 7. Suppose \mathcal{D} is a differential operator with polynomial coefficients, and the numerical solution $T_r(\zeta)$ is defined on the knot grid $T^\rho \subset \Omega_0 \subset \mathbb{R}^d$. If $\mathcal{D}T_r(\zeta) = \frac{P_k(\zeta)}{W_k(\zeta)}$ is an interpolant of $\mathcal{D}T(\zeta)$, and $W_k(\zeta)\mathcal{D}T(\zeta) \in W_p^m(\Omega_0)$, we have

$$\|\mathcal{D}T(\zeta) - \mathcal{D}T_r(\zeta)\|_{L^\infty} \leq C_I \rho^{m-d/p} \left\| \frac{1}{W_k(\zeta)} \right\|_{L^\infty},$$

where ρ is the knot grid size of T^ρ which $T_r(\zeta)$ is defined on, and $C_I > 0$ is a constant independent of ρ .

4.2. Convergence

In this subsection, we present a theoretical result on convergence of the IGA-C method. That is, if the differential operator in \mathcal{D} (1) is stable or strongly monotone, the corresponding IGA-C method is convergent.

Definition 2 (Stability estimate and stable operator [24]). Let V, W be Hilbert spaces and $\mathcal{D} : V \rightarrow W$ a differential operator. If there exists a constant $C_S > 0$ such that,

$$\|\mathcal{D}v\|_W \geq C_S \|v\|_V, \quad \text{for all } v \in D(\mathcal{D}), \tag{16}$$

where $D(\mathcal{D})$ represents the domain of \mathcal{D} , the differential operator \mathcal{D} is called the stable operator, and the inequality (16) is called the stability estimate.

Remark 3. In this subsection, we suppose that the L^∞ norm $\|\cdot\|_{L^\infty}$ is equivalent to the norm $\|\cdot\|_V$ in V , and the norm $\|\cdot\|_W$ in W . In other words, there exist nonnegative constants c_V, C_V, c_W , and C_W satisfying

$$\begin{aligned} c_V \|\cdot\|_V &\leq \|\cdot\|_{L^\infty} \leq C_V \|\cdot\|_V, \\ c_W \|\cdot\|_W &\leq \|\cdot\|_{L^\infty} \leq C_W \|\cdot\|_W. \end{aligned}$$

Theorem 8. Suppose NURBS function T_r is the numerical solution to the boundary value problem (1), generated by the IGA-C method. If the differential operator $\mathcal{D} : V \rightarrow W$ in (1) is a stable operator and T_r satisfies the local Lipschitz condition, T_r will converge to the analytic solution T , when each knot interval of T_r tends to a point.

Proof. The differential operator \mathcal{D} in (1) is a stable operator, so there exists a constant $C_S > 0$, such that

$$\|\mathcal{D}(T - T_r)\|_W \geq C_S \|T - T_r\|_V.$$

And it is equivalent to

$$\|T - T_r\|_V \leq \frac{1}{C_S} \|\mathcal{D}T - \mathcal{D}T_r\|_W.$$

Due to the equivalence of $\|\cdot\|_{L^\infty}$ and $\|\cdot\|_W$, and the consistency of the IGA-C method (Theorems 4–6), this theorem is proved. \square

Moreover, we have,

Theorem 9. Suppose NURBS function T_r is the numerical solution to the boundary value problem (1), generated by the IGA-C method. If the differential operator $\mathcal{D} : V \rightarrow W$ in (1) is a stable operator with polynomial coefficients, and the conditions of Theorem 7 are satisfied, then the error bound between the analytic solution T and the numerical solution T_r fulfills,

$$\|T - T_r\|_V \leq C_\mathcal{L} \rho^{m-d/p} \left\| \frac{1}{W_k(\zeta)} \right\|_{L^\infty},$$

where ρ is the knot grid size of \mathcal{T}^ρ which T_r is defined on, and $C_\mathcal{L}$ is a constant independent of ρ .

Theorem 9 can be proved directly based on Theorem 7 and Definition 2.

Definition 3 (Strongly monotone operator [24]). Let V be a Hilbert space and $\mathcal{D} \in \mathcal{L}(V, V')$. The operator \mathcal{D} is said to be a strongly monotone operator, if there exists a constant $C_D > 0$, such that,

$$\langle \mathcal{D}v, v \rangle \geq C_D \|v\|_V^2, \text{ for all } v \in V. \tag{17}$$

For every $v \in V$, the element $\mathcal{D}v \in V'$ is a linear form. The symbol $\langle \mathcal{D}v, v \rangle$, which means the application of $\mathcal{D}v$ to $v \in V$, is called duality pairing.

Lemma 4. Let V be a Hilbert space and $\mathcal{D} \in \mathcal{L}(V, V')$ a continuous strongly monotone linear operator. Then there exists a constant $C_D > 0$ such that \mathcal{D} satisfies the stability estimate (16) [24].

Proof. The strong monotonicity condition (17) implies,

$$C_D \|v\|_V^2 \leq \langle \mathcal{D}v, v \rangle \leq \|\mathcal{D}v\|_{V'} \|v\|_V,$$

which means

$$C_D \|v\|_V \leq \|\mathcal{D}v\|_{V'}. \quad \square$$

Consequently, we have the following corollary.

Corollary 2. Suppose NURBS function T_r is the numerical solution to the boundary value problem (1), generated by the IGA-C method, and the norm $\|\cdot\|_{L^\infty}$ bounds the norm $\|\cdot\|_{V'}$. If the differential operator \mathcal{D} in (1) is a strongly monotone operator, and T_r satisfies the local Lipschitz condition, then T_r will converge to the analytic solution T , when each knot interval of T_r tends to a point.

This is a direct corollary of Lemma 4 and Theorem 8.

Based on Theorem 9 and Lemma 4, we also have,

Corollary 3. Suppose NURBS function T_r is the numerical solution to the boundary value problem (1), generated by the IGA-C method, and the norm $\|\cdot\|_{L^\infty}$ bounds the norm $\|\cdot\|_{V'}$. If the differential operator \mathcal{D} in (1) is a strongly monotone operator with polynomial coefficients, and the conditions of Theorem 7 are satisfied, the following error bound formula holds, i.e.,

$$\|T - T_r\|_V \leq C_\mathcal{M} \rho^{m-d/p} \left\| \frac{1}{W_k(\zeta)} \right\|_{L^\infty},$$

where T is the analytical solution to the problem (1), ρ is the knot grid size of \mathcal{T}^ρ which T_r is defined on, and $C_\mathcal{M}$ is a constant independent of ρ .

Remark 4. It is well known that a wide class of elliptic differential operators are stable or strongly monotone. So the IGA-C method for equations with these elliptic differential operators is convergent.

4.3. Examples

In this subsection, we give two examples of PDE whose differential operators are strongly monotone. So the IGA-C method for them is convergent. Both examples can also be found in Ref. [24]. Further, a 2D and a 3D numerical examples are presented in Sections 4.3.2 and 4.3.3, respectively.

4.3.1. Examples of strongly monotone operator

Example 1. Consider the following boundary value problem:

$$\begin{cases} \mathcal{D}u = -\nabla \cdot (a_1 \nabla u) + a_0 u = f & \text{in } \Omega \\ u(x) = 0 & \text{on } \partial\Omega \end{cases} \tag{18}$$

where $a_1(x) \geq C_{min} > 0$, $a_0(x) \geq 0$.

The weak formulation of this boundary value problem is stated as follows:

Let $V = H_0^1(\Omega) = \{v \in W^{1,2}(\Omega); v = 0 \text{ on } \partial\Omega\}$, where $W^{1,2}(\Omega)$ is a Sobolev space, and define a bilinear form $a(\cdot, \cdot) : V \times V \rightarrow \mathbb{R}$,

$$a(u, v) = \int_{\Omega} (a_1 \nabla u \cdot \nabla v + a_0 u v) dx,$$

associated with a unique linear operator $\mathcal{D} : V \rightarrow V'$ defined by

$$\langle \mathcal{D}u, v \rangle = a(u, v) \quad \text{for all } u, v \in V$$

and a linear form $l \in V'$,

$$l(v) = \int_{\Omega} f v dx.$$

Find a function $u \in V$ such that

$$a(u, v) = l(v) \quad \text{for all } v \in V.$$

Next, we will prove that this differential operator is strongly monotone. According to the Poincaré–Friedrichs' inequality [24] in the space $V = H_0^1(\Omega)$, we have

$$|v|_{1,2} \leq \|v\|_{1,2} \leq C^{-1} |v|_{1,2} \quad \text{for all } v \in V,$$

where $C > 0$ is a constant, $|v|_{1,2} = (\int_{\Omega} |\nabla v|^2 dx)^{\frac{1}{2}}$ is a seminorm, and the norm $\|v\|_{1,2}$ is generated by adding a nonnegative term to the seminorm $|v|_{1,2}$ [24]. Also noticing that $a_1(x) \geq C_{min} > 0$ and $a_0(x) \geq 0$, we obtain that

$$a(v, v) = \int_{\Omega} (a_1 |\nabla v|^2 + a_0 v^2) dx \geq \int_{\Omega} a_1 |\nabla v|^2 dx \geq C_{min} \int_{\Omega} |\nabla v|^2 dx = C_{min} |v|_{1,2}^2 \geq C_{min} C^2 \|v\|_{1,2}^2 \quad \text{for all } v \in V.$$

Using the inequality

$$\|v\|_V \leq \|v\|_{1,2},$$

we have

$$\langle \mathcal{D}v, v \rangle \geq C_{min} C^2 \|v\|_{1,2}^2 \geq C_{min} C^2 \|v\|_V^2.$$

By Definition 2, the operator \mathcal{D} is proved to be a strongly monotone operator. Therefore, suppose the norm $\|\cdot\|_{L^\infty}$ bounds the norm $\|\cdot\|_{V'}$, the IGA-C method for the boundary value problem (18) is convergent, if the generated numerical solution satisfies the local Lipschitz condition, or \mathcal{D} is a operator with polynomial coefficients.

Remark 5. This partial differential problem is fairly general, and it can describe a wide range physical processes, such as stationary heat transfer, electrostatics, transverse deflection of a cable, axial deformation of a bar, pipe flow, laminar incompressible flow through a channel under constant pressure gradient, and porous media flow, and so on.

Example 2. The heat transfer equation with homogeneous Dirichlet boundary condition is represented by

$$\begin{cases} \mathcal{D}u = \frac{\partial u}{\partial t} - \Delta u = f & \text{in } \Omega \\ u(0) = u_0 & \text{on } \partial\Omega \end{cases} \tag{19}$$

This is a linear parabolic differential equation with homogenous Dirichlet boundary condition. And this differential operator is strongly monotone [24]. Therefore, suppose the norm $\|\cdot\|_{L^\infty}$ bounds the norm $\|\cdot\|_{V'}$, the IGA-C method for the boundary value problem (19) is convergent, if the generated numerical solution satisfies the local Lipschitz condition, or \mathcal{D} is a operator with polynomial coefficients.

Table 4
Statistics on the convergence of relative errors vs. number of control points

| Example in 2D | | | Example in 3D | | |
|---------------------|--------|----------|---------------------|--------|----------|
| Number ^a | e_T | e_{DT} | Number ^a | e_T | e_{DT} |
| 4 × 4 | 0.5464 | 1.1730 | 4 × 4 × 4 | 1.2075 | 1.8073 |
| 5 × 5 | 0.2682 | 0.3290 | 5 × 5 × 5 | 0.3579 | 0.5746 |
| 6 × 6 | 0.3891 | 0.3377 | 5 × 5 × 6 | 0.2990 | 0.5023 |
| 7 × 7 | 0.1780 | 0.1483 | 5 × 6 × 6 | 0.2299 | 0.4003 |
| 8 × 8 | 0.1064 | 0.0983 | 6 × 6 × 6 | 0.1394 | 0.2261 |
| 9 × 9 | 0.0704 | 0.0674 | 7 × 7 × 7 | 0.1546 | 0.1848 |
| 10 × 10 | 0.0050 | 0.0497 | 8 × 8 × 8 | 0.1129 | 0.1266 |
| 12 × 12 | 0.0291 | 0.0307 | 9 × 9 × 9 | 0.0832 | 0.0946 |
| 13 × 13 | 0.0233 | 0.0251 | 10 × 10 × 10 | 0.0628 | 0.0578 |
| 14 × 14 | 0.0191 | 0.0209 | 11 × 11 × 11 | 0.0491 | 0.0550 |
| 15 × 15 | 0.0159 | 0.0178 | 12 × 12 × 12 | 0.0392 | 0.0417 |
| 17 × 17 | 0.0116 | 0.0132 | 13 × 13 × 13 | 0.0320 | 0.0346 |
| 19 × 19 | 0.0088 | 0.0104 | 14 × 14 × 14 | 0.0265 | 0.0283 |

^a Number of control points.

Before showing numerical examples in Sections 4.3.2 and 4.3.3, we define two relative errors to measure the approximation precision, i.e., the *relative error for T*,

$$e_T = \sqrt{\frac{\int_{\Omega} (T - T_r)^t (T - T_r) d\Omega}{\int_{\Omega} T^t T d\Omega}} \quad (20)$$

and the *relative error for DT*

$$e_{DT} = \sqrt{\frac{\int_{\Omega} (DT - DT_r)^t (DT - DT_r) d\Omega}{\int_{\Omega} (DT)^t (DT) d\Omega}}. \quad (21)$$

Additionally, for illustrating the error distribution of the numerical solution, the following absolute error e_a is employed, i.e.,

$$\begin{aligned} e_a(u, v) &= |T(u, v) - T_r(u, v)|, \text{ for 2D case,} \\ e_a(u, v, w) &= |T(u, v, w) - T_r(u, v, w)|, \text{ for 3D case.} \end{aligned} \quad (22)$$

4.3.2. Numerical example in 2-dimension

Consider a source problem on a 2D domain Ω ,

$$\begin{cases} -\Delta T + T = f, & (x, y) \in \Omega \\ T|_{\partial\Omega} = 0, \end{cases} \quad (23)$$

where the 2D domain Ω is a quarter of an annulus, which can be exactly represented by a cubic NURBS patch with 4×4 control points, presented in Appendix A.1, and

$$f = (3x^4 - 67x^2 - 67y^2 + 3y^4 + 6x^2y^2 + 116) \sin(x) \sin(y) + (68x - 8x^3 - 8xy^2) \cos(x) \sin(y) + (68y - 8y^3 - 8yx^2) \cos(y) \sin(x).$$

The analytical solution of the source problem (23) is (see Fig. 2(a)),

$$T = (x^2 + y^2 - 1)(x^2 + y^2 - 16) \sin(x) \sin(y).$$

Clearly, Eq. (23) is a special case of Example 1, and the operator in Eq. (23) is a strongly monotone operator with constant coefficients. So the IGA-C method is convergent for the 2D source problem (23).

To solve the problem (23) with the IGA-C method, we uniformly insert 15 knots along u - and v -directions, respectively, to the cubic NURBS patch presented in Appendix A.1, and obtain a cubic NURBS patch with 19×19 control points. Then this problem can be solved with the IGA-C method, by taking Greville abscissae as collocation points.

The relative errors e_T and e_{DT} with the increasing number of control points are listed in Table 4. For clarity, we illustrate the diagram of the logarithm (base 10) of the relative error v.s. the number of the control points in Fig. 1(a), where x -axis is the number of control points, and y -axis represents the logarithm (base 10) of the relative errors. In this figure, the diagram of the logarithm (base 10) of e_T (20) v.s. the number of the control points is in blue, and that of e_{DT} (21) v.s. the number of the control points is in red.¹ From the data listed in Table 4 and the diagrams illustrated in Fig. 1(a), we can see that the convergence rates of T_r and DT_r are nearly the same.

¹ For interpretation of color in Fig. 1, the reader is referred to the web version of this article.

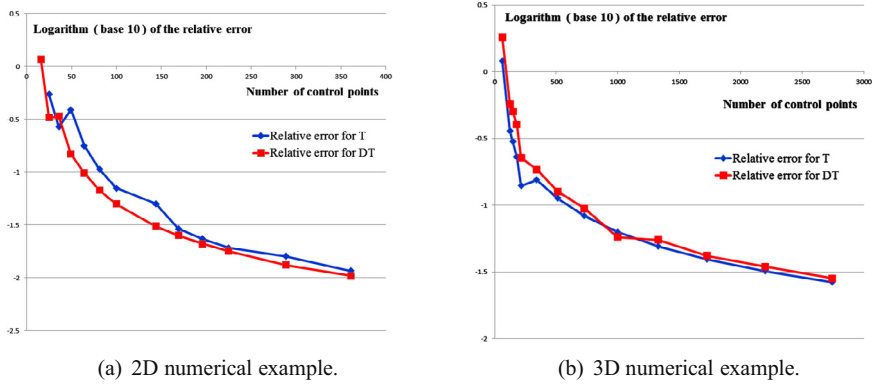


Fig. 1. Diagram of the relative error (logarithm base 10) v.s. the number of the control points.

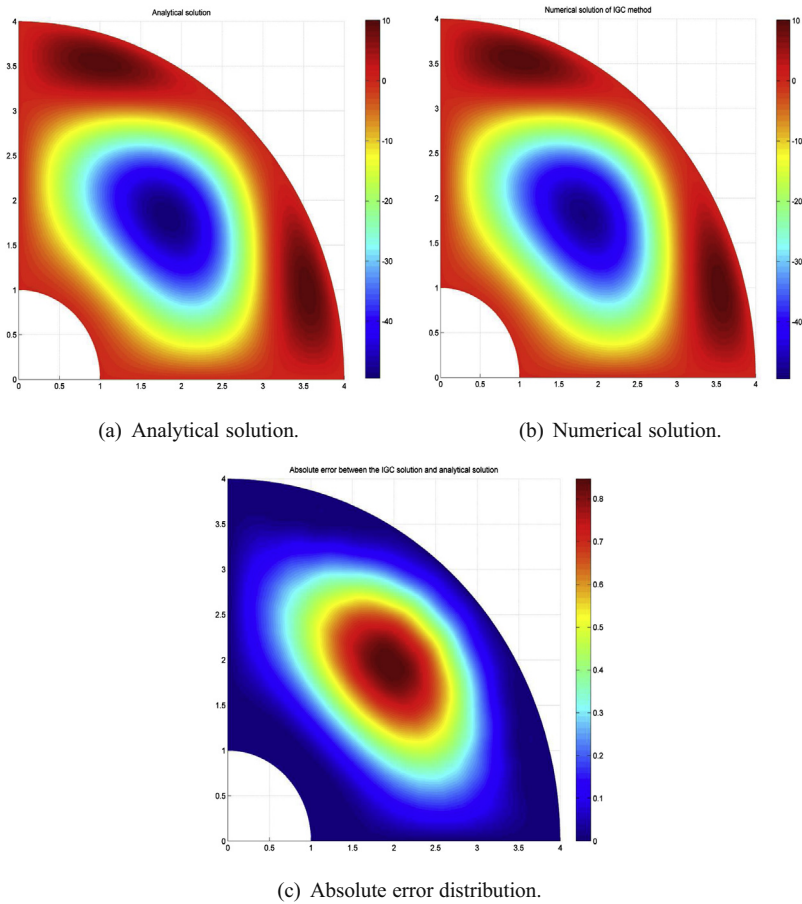


Fig. 2. Analytical solution (a), numerical solution (b) and the absolute error distribution diagram (c) in the 2D numerical example when the number of control points is 15×15 .

Moreover, we demonstrate the analytical solution of the 2D source problem (23) in Fig. 2(a). Fig. 2(b) is the numerical solution with 15×15 control points, and Fig. 2(c) is its absolute error distribution. The relative errors of the numerical solution in Fig. 2(b) are $e_T = 0.0159$ and $e_{DT} = 0.0178$,

4.3.3. Numerical example in 3-dimension

This numerical example is a source problem defined on 3D cubic domain $\Omega = [0, 1] \times [0, 1] \times [0, 1]$, i.e.,

$$\begin{cases} -\Delta T + T = f, & (x, y, z) \in \Omega, \\ T|_{\partial\Omega} = 0, \end{cases} \quad (24)$$

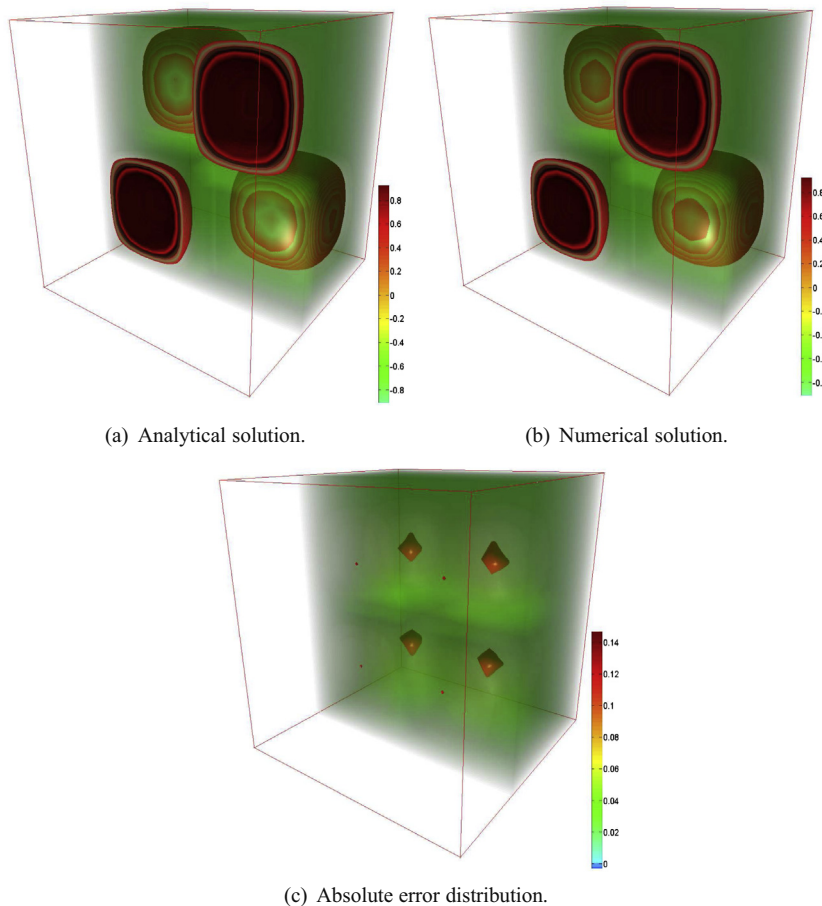


Fig. 3. Analytical solution (a), numerical solution (b) and the absolute error distribution diagram (c) in the 3D numerical example when the number of control points is $10 \times 10 \times 10$.

where

$$f = (1 + 12\pi^2) \sin(2\pi x) \sin(2\pi y) \sin(2\pi z).$$

The analytical solution is (see Fig. 3(a)),

$$T = \sin(2\pi x) \sin(2\pi y) \sin(2\pi z).$$

According to the analysis in Section 4.3.1, the operator in Eq. (24) is a strongly monotone operator with constant coefficients, and then the IGA-C method is convergent for the source problem (24) in 3D.

To solve the source problem (24) with the IGA-C method, its 3D physical domain Ω is modeled as a cubic B-spline solid with $4 \times 4 \times 4$ control points, listed in Appendix A2. Then, along x -, y -, and z -directions, 10 knots are uniformly inserted, respectively, to generate a cubic B-spline solid with $14 \times 14 \times 14$ control points. Accordingly, the analytical solution of Eq. (24) is approximated by cubic B-spline functions with $4 \times 4 \times 4$ to $14 \times 14 \times 14$ unknown control coefficients (refer to Table 4), respectively. Fig. 3(b) illustrates the numerical solution generated by the IGA-C method with $10 \times 10 \times 10$ control points, where $e_T = 0.0628$ and $e_{DT} = 0.0578$, and Fig. 3(c) is the absolute error distribution diagram.

Moreover, the statistics of the relative errors (e_T and e_{DT}) v.s. the number of control points are listed in Table 4, and the diagrams of the logarithm (base 10) of the relative errors v.s. the number of control points are demonstrated in Fig. 1(a). It shows once again that the convergence rates of T_r and DT_r are nearly the same.

5. Conclusion

The IGA method approximates the solution of a boundary value problem (or initial value problem) with a NURBS function T_r . The IGA-C method solves the NURBS function T_r by making the approximate differential operator interpolate the analytical differential operator at collocation points. In this paper, we first prove that NURBS function T_r , its (partial) derivatives of arbitrary order, and DT_r all have the same knot intervals. Next, we show the consistency of the IGA-C method, i.e., the

Table 5
Control points of the quarter of annulus.

| i | $B_{i,1}$ | $B_{i,2}$ | $B_{i,3}$ | $B_{i,4}$ |
|-----|--------------------|---------------------|---------------------|---------------------|
| 1 | (1,0) | (2,0) | (3,0) | (4,0) |
| 2 | $(1,2 - \sqrt{2})$ | $(2,4 - 2\sqrt{2})$ | $(3,6 - 3\sqrt{2})$ | $(4,8 - 4\sqrt{2})$ |
| 3 | $(2 - \sqrt{2},1)$ | $(4 - 2\sqrt{2},2)$ | $(6 - 3\sqrt{2},3)$ | $(8 - 4\sqrt{2},4)$ |
| 4 | (0,1) | (0,2) | (0,3) | (0,4) |

Table 6
Weights for the quarter of annulus.

| i | $\omega_{i,1}$ | $\omega_{i,2}$ | $\omega_{i,3}$ | $\omega_{i,4}$ |
|-----|------------------------|------------------------|------------------------|------------------------|
| 1 | 1 | 1 | 1 | 1 |
| 2 | $\frac{1+\sqrt{2}}{3}$ | $\frac{1+\sqrt{2}}{3}$ | $\frac{1+\sqrt{2}}{3}$ | $\frac{1+\sqrt{2}}{3}$ |
| 3 | $\frac{1+\sqrt{2}}{3}$ | $\frac{1+\sqrt{2}}{3}$ | $\frac{1+\sqrt{2}}{3}$ | $\frac{1+\sqrt{2}}{3}$ |
| 4 | 1 | 1 | 1 | 1 |

Table 7
Control points of the cubic B-spline solid.

| i | j | $B_{ij,1}$ | $B_{ij,2}$ | $B_{ij,3}$ | $B_{ij,4}$ |
|-----|-----|-------------|---------------|---------------|-------------|
| 1 | 1 | (0,0,0) | (0,0,1/3) | (0,0,2/3) | (0,0,1) |
| 1 | 2 | (0,1/3,0) | (0,1/3,1/3) | (0,1/3,2/3) | (0,1/3,1) |
| 1 | 3 | (0,2/3,0) | (0,2/3,1/3) | (0,2/3,2/3) | (0,2/3,1) |
| 1 | 4 | (0,1,0) | (0,1,1/3) | (0,1,2/3) | (0,1,1) |
| 2 | 1 | (1/3,0,0) | (1/3,0,1/3) | (1/3,0,2/3) | (1/3,0,1) |
| 2 | 2 | (1/3,1/3,0) | (1/3,1/3,1/3) | (1/3,1/3,2/3) | (1/3,1/3,1) |
| 2 | 3 | (1/3,2/3,0) | (1/3,2/3,1/3) | (1/3,2/3,2/3) | (1/3,2/3,1) |
| 2 | 4 | (1/3,1,0) | (1/3,1,1/3) | (1/3,1,2/3) | (1/3,1,1) |
| 3 | 1 | (2/3,0,0) | (2/3,0,1/3) | (2/3,0,2/3) | (2/3,0,1) |
| 3 | 2 | (2/3,1/3,0) | (2/3,1/3,1/3) | (2/3,1/3,2/3) | (2/3,1/3,1) |
| 3 | 3 | (2/3,2/3,0) | (2/3,2/3,1/3) | (2/3,2/3,2/3) | (2/3,2/3,1) |
| 3 | 4 | (2/3,1,0) | (2/3,1,1/3) | (2/3,1,2/3) | (2/3,1,1) |
| 4 | 1 | (1,0,0) | (1,0,1/3) | (1,0,2/3) | (1,0,1) |
| 4 | 2 | (1,1/3,0) | (1,1/3,1/3) | (1,1/3,2/3) | (1,1/3,1) |
| 4 | 3 | (1,2/3,0) | (1,2/3,1/3) | (1,2/3,2/3) | (1,2/3,1) |
| 4 | 4 | (1,1,0) | (1,1,1/3) | (1,1,2/3) | (1,1,1) |

approximate differential expression \mathcal{DT}_r will tend to the real differential expression \mathcal{DT} , when each knot interval of T_r tends to a point. A theoretical result on the convergence of the IGA-C method is also established. We show that, if the differential operator is stable or strongly monotone, the corresponding IGA-C method is convergent. Since a wide class of differential operators are stable or strongly monotone, the IGA-C method is convergent for them.

Acknowledgments

We thank Prof. Daoyuan Fang from Department of Mathematics, Zhejiang University for his help in preparing this paper. This work is supported by the Natural Science Foundation of China (Nos. 61379072, 61202201, 60933008, 60970150). Dr. Qianqian Hu is also supported by the Open Project Program (No. A1305) of the State Key Lab of CAD&CG, Zhejiang University.

Appendix A. Appendix

In the Appendix, we list the control points, knot vector, and weights of the NURBS representation of the physical domains in the two numerical examples.

A.1. NURBS representation of the physical domain in the 2D numerical example in Section 4.3.2

The physical domain in the 2D numerical example presented in Section 4.3.2 is represented by a cubic NURBS patch. Its control points are listed in the following [Tables 5 and 6](#) presents its weights.

The knot vectors along u - and v -direction are, respectively,

$$\begin{array}{cccccccc} 0 & 0 & 0 & 0 & 1 & 1 & 1 & 1, \\ 0 & 0 & 0 & 0 & 1 & 1 & 1 & 1. \end{array}$$

A.2. B-spline representation of the physical domain in the 3D numerical example in Section 4.3.3

The physical domain in the 3D numerical example presented in Section 4.3.3 is represented by a cubic B-spline solid. Its control points are listed in the following Table 7.

The knot vectors along u -, v -, and w -directions are, respectively,

$$\begin{array}{cccccccc} 0 & 0 & 0 & 0 & 1 & 1 & 1 & 1, \\ 0 & 0 & 0 & 0 & 1 & 1 & 1 & 1, \\ 0 & 0 & 0 & 0 & 1 & 1 & 1 & 1. \end{array}$$

References

- [1] T. Hughes, J. Cottrell, Y. Bazilevs, Isogeometric analysis: Cad, finite elements, nurbs, exact geometry and mesh refinement, *Computer Methods in Applied Mechanics and Engineering* 194 (39) (2005) 4135–4195.
- [2] F. Auricchio, L. Beirão da Veiga, A. Buffa, C. Lovadina, A. Reali, G. Sangalli, A fully locking-free isogeometric approach for plane linear elasticity problems: a stream function formulation, *Computer Methods in Applied Mechanics and Engineering* 197 (1) (2007) 160–172.
- [3] T. Elguedj, Y. Bazilevs, V. Calo, T. Hughes, \bar{B} and \bar{F} projection methods for nearly incompressible linear and non-linear elasticity and plasticity using higher-order nurbs elements, *Computer Methods in Applied Mechanics and Engineering* 197 (2008) 2732–2762.
- [4] J. Cottrell, A. Reali, Y. Bazilevs, T. Hughes, Isogeometric analysis of structural vibrations, *Computer Methods in Applied Mechanics and Engineering* 195 (41) (2006) 5257–5296.
- [5] T. Hughes, A. Reali, G. Sangalli, Duality and unified analysis of discrete approximations in structural dynamics and wave propagation: comparison of p -method finite elements with k -method nurbs, *Computer Methods in Applied Mechanics and Engineering* 197 (49) (2008) 4104–4124.
- [6] W. Wall, M. Frenzel, C. Cyron, Isogeometric structural shape optimization, *Computer Methods in Applied Mechanics and Engineering* 197 (33) (2008) 2976–2988.
- [7] Y. Bazilevs, V. Calo, T. Hughes, Y. Zhang, Isogeometric fluid-structure interaction: theory, algorithms, and computations, *Computational Mechanics* 43 (1) (2008) 3–37.
- [8] Y. Bazilevs, V. Calo, Y. Zhang, T. Hughes, Isogeometric fluid-structure interaction analysis with applications to arterial blood flow, *Computational Mechanics* 38 (4) (2006) 310–322.
- [9] Y. Bazilevs, J. Gohean, T. Hughes, R. Moser, Y. Zhang, Patient-specific isogeometric fluid-structure interaction analysis of thoracic aortic blood flow due to implantation of the jarvik 2000 left ventricular assist device, *Computer Methods in Applied Mechanics and Engineering* 198 (45) (2009) 3534–3550.
- [10] Y. Bazilevs, L. Beirão da Veiga, J. Cottrell, T. Hughes, G. Sangalli, Isogeometric analysis: approximation, stability and error estimates for h -refined meshes, *Mathematical Models and Methods in Applied Sciences* 16 (07) (2006) 1031–1090.
- [11] J. Cottrell, T. Hughes, A. Reali, Studies of refinement and continuity in isogeometric structural analysis, *Computer Methods in Applied Mechanics and Engineering* 196 (41) (2007) 4160–4183.
- [12] T. Hughes, A. Reali, G. Sangalli, Efficient quadrature for nurbs-based isogeometric analysis, *Computer Methods in Applied Mechanics and Engineering* 199 (5) (2010) 301–313.
- [13] M. Aigner, C. Heinrich, B. Jüttler, E. Pilgerstorfer, B. Simeon, A. Vuong, Swept volume parameterization for isogeometric analysis, *Mathematics of Surfaces XIII* (2009) 19–44.
- [14] G. Xu, B. Mourrain, R. Duvigneau, A. Galligo, Optimal analysis-aware parameterization of computational domain in 3d isogeometric analysis, *Computer-Aided Design* 45 (4) (2013) 812–821.
- [15] G. Xu, B. Mourrain, R. Duvigneau, A. Galligo, Parameterization of computational domain in isogeometric analysis: methods and comparison, *Computer Methods in Applied Mechanics and Engineering* 200 (23) (2011) 2021–2031.
- [16] J. Cottrell, T. Hughes, Y. Bazilevs, *Isogeometric Analysis: Toward Integration of CAD and FEA*, Wiley, 2009.
- [17] F. Auricchio, L. Beirão da Veiga, T. Hughes, A. Reali, G. Sangalli, Isogeometric collocation methods, *Mathematical Models and Methods in Applied Sciences* 20 (11) (2010) 2075–2107.
- [18] F. Auricchio, L. Beirão da Veiga, T. Hughes, A. Reali, G. Sangalli, Isogeometric collocation for elastostatics and explicit dynamics, *Computer Methods in Applied Mechanics and Engineering* 249 (2012) 2–14.
- [19] L. Beirão da Veiga, C. Lovadina, A. Reali, Avoiding shear locking for the timoshenko beam problem via isogeometric collocation methods, *Computer Methods in Applied Mechanics and Engineering* 241 (2012) 38–51.
- [20] F. Auricchio, L. Beirão da Veiga, J. Kiendl, C. Lovadina, A. Reali, Locking-free isogeometric collocation methods for spatial timoshenko rods, *Computer Methods in Applied Mechanics and Engineering* 263 (15) (2013) 113–126.
- [21] D. Schillinger, J.A. Evans, A. Reali, M.A. Scott, T.J. Hughes, Isogeometric collocation: cost comparison with Galerkin methods and extension to adaptive hierarchical NURBS discretizations, *Computer Methods in Applied Mechanics and Engineering* 267 (2013) 170–232.
- [22] X. Chen, R.F. Riesenfeld, E. Cohen, Sliding windows algorithm for b-spline multiplication, in: *Proceedings of the 2007 ACM Symposium on Solid and Physical Modeling*, ACM, 2007, pp. 265–276.
- [23] S.C. Brenner, L.R. Scott, *The Mathematical Theory of Finite Element Methods*, third ed., vol. 15, Springer, 2008.
- [24] P. Solin, *Partial Differential Equations and the Finite Element Method*, Wiley-Interscience, 2006.